sck cen

Registered Office
Herrmann-Debrouxlaan 40
1160 Brussel – Belgium

Foundation of Public Utility
VAT BE 406.568.867

Research Centres
Boeretang 200
2400 Mol – Belgium

Chemin du Cyclotron 6
1348 Ottignies-Louvain-la-Neuve – Belgium

Reference N°	Creation Date	
SCK CEN/46654602	2021-12-13	
Alternative Reference N°	Revision	Version
N/A	1.0	1
ISC	Revision Status	
Restricted	Approved	

Borella A. et al_paper_JNMM_2021_Peak Shape Characterization of a 500 mm3 Cadmium Zinc Telluride Detector and Analysis of Spectroscopic Measurement Data for Uranium Samples

Authors*
Alessandro Borella

Approval information for current revision*		
Name	**Outcome**	**Date**
Sonja Ruts	Approved	2022-01-05

Change log*				
Revision	**Version**	**Status**	**Date**	**Description of change**
1.0	1	Approved	2021-12-13	

**This automatically generated cover page shows references and document information as were available in the Alexandria document management system on 2022-01-05. Please refer to Alexandria for current and complete metadata, or to the document contents and/or author for additional information.*

Exploring
a better tomorrow

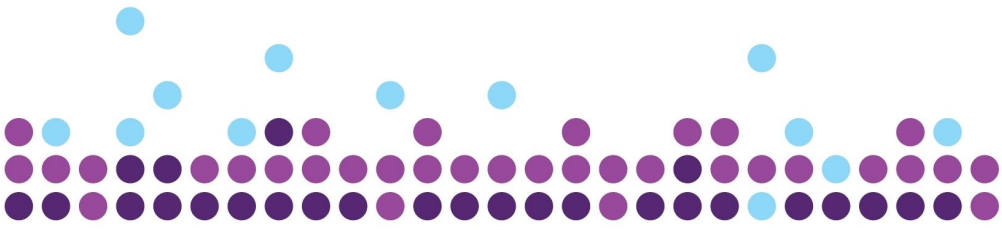

Peak Shape Characterization of a 500 mm^3 Cadmium Zinc Telluride Detector and Analysis of Spectroscopic Measurement Data for Uranium Samples

Alessandro Borella, Michel Bruggeman, Riccardo Rossa, Peter Schillebeeckx, and Tim Vidmar

Abstract

Gamma-ray spectra of calibrated sources and reference standard samples of uranium were recorded with a 500 mm^3 Cadmium Zinc Telluride (CZT) detector. The measurements with calibrated sources were used to set up the peak-shape calibration of the CZT detector as a function of the deposited energy and the obtained net peak areas were compared with the ones obtained with Monte Carlo modelling. The obtained calibrations were then used to determine net peak areas in spectra measured of low-enriched uranium standard samples with the aim to determine their uranium enrichment with the "peak-ratio method." The results of the analyses of different samples show that both the net peak area of the 0.258 MeV gamma ray and the intrinsic detector efficiency have a strong impact on the determined enrichment. In addition, the impact of the values of gamma-ray emission probabilities from different data libraries was also studied.

KEYWORDS
CZT, cadmium zinc telluride, medium resolution gamma-ray spectroscopy, peak shape, safeguards, nondestructive assay, nuclear data

Introduction

Cadmium Zinc Telluride (CZT) detectors are room temperature solid state gamma-ray detectors. The full-energy peak shapes of CZT detectors exhibit a low energy tail due to mechanisms related to the charge transport in the crystal.[1,2] Their counting efficiency is limited since the production of crystals larger than a few cm^3 is difficult and negatively impacts the energy resolution. In^3 for a detector size up to 19 cm^3 a resolution of less than 1%, expressed in full width at half maximum (FWHM), for the 0.662 MeV full energy peak, was reported. Given their compact size, portability and good energy resolution, CZT detectors can be deployed in many applications, such as attribute testing for fresh and irradiated nuclear material during safeguards inspections.[4,5]

In this paper we first report about the peak-shape calibration of a 500 mm^3 CZT detector with a nominal resolution of 1.3%.[6] The peak shape parameters were expressed as analytical functions of energy implemented in a peak fitting algorithm. This peak fitting algorithm was then used to determine the net peak areas in spectra recorded with certified uranium standards.[7]

The so-called "peak ratio" method was then used to determine the uranium enrichment in these standards. The dependence of the counting efficiency of the standards on the gamma ray energy was obtained from Monte Carlo simulations. The Monte Carlo model of the detector was validated beforehand using measurements with calibrated point sources. We also discuss the impact of nuclear data and the inclusion of the 0.258 MeV gamma ray on the calculated uranium enrichment.

The uncertainties in this paper are quoted at a 68% confidence limit. We quote the uncertainties between parentheses as recommended later.[8]

Peak Shape Calibration

In the Borella 2021 paper,[7] the peak shape of a CZT detector was described by a Gaussian function in combination with a low energy tail, as originally proposed in (equation no. 1)[9]:

$$R(E_d) = \frac{C}{1+A_T}\left(\frac{1}{\sqrt{2\pi}\sigma_E}exp\left(-\frac{(E_d-\mu)^2}{2\sigma_E^2}\right)+\frac{1}{2}\frac{A_T}{\tau_E^{\square}}exp\left(\frac{E_d-\mu}{\tau_E^{\square}}+\frac{1}{2}\frac{\sigma_E^2}{\tau_E^2}\right)erfc\left(\frac{E_d-\mu}{\sqrt{2}\sigma_E^{\square}}+\frac{\sigma_E^{\square}}{\sqrt{2}\tau_E^{\square}}\right)\right)$$

Where:

- C is the net peak area
- E_d is the observed signal
- the peak position is indicated by m
- represents the variance of the Gaussian component
- t_E indicates the slope of the exponential tail
- A_T is the area of the tail component relative to the one of the Gaussian function
- the term *erfc* is the complementary error function

The tailing effect is treated in a phenomenological way by using a function similar to the one typically used for other semi-conductor detectors.[9] We first determined the peak shape parameters from experimental data obtained with calibrated sources in energy regions of the spectra with no or very little peak overlap. These regions were constrained by the user to allow including the low energy tail. The region boundaries are increasingly asymmetrical with respect to the gamma-ray peak position as the gamma ray energy increases.

Measurements with calibrated point sources with gamma energies between 0.06 MeV and 1.33 MeV were carried out and from the analysis of well isolated peaks it was found[7] that the energy calibration, linking *m* and the gamma ray energy *E* can be described by a linear function; that the variance of the Gaussian can be described by a parabolic function of the gamma ray energy; that the slope of the tail can be modelled by a linear function of the gamma ray energy; and that the relative area of the tail follows an exponential behaviour towards an asymptotic value.

The result of this fitting procedure for the 0.835 MeV gamma-ray peak of ^{54}Mn is shown in Figure 1.

A least-square multi-peak fitting algorithm was then implemented where the peak shape defined by equation 1 and the predefined energy dependence of the peak shape parameters were used. The background in the region of a full energy peak at energy *E* was parameterised by a sum of a step function of height *H* and a constant *B* (equation no. 2):

$$\frac{H}{2}\left(1 - erf\left(\frac{E_d - \mu}{\sqrt{2}\sigma_\mu}\right)\right) + B$$

Monte Carlo Model

The net peak areas of the well isolated peaks obtained from the spectra of the calibrated sources used for the determination of the peak shape calibration were also used to validate the Monte Carlo model of the detector. The measurements were carried out in an open geometry without any collimator and with the sources positioned at a fixed distance of about 30 mm from the CZT detector holder. The signal processing and readout were all the same for the considered sources. Given the fact that the count rate was at most 120 count/s we do not expect a significant impact due to pile-up events on the measured net peak areas.

A first analysis[7] revealed that the counting efficiency obtained by Monte Carlo simulations was overestimated above 0.15 MeV and underestimated below 0.15 MeV, compared with the experimental counting efficiency.

The detector crystal was modelled as a 5 mm x 10 mm x 10 mm rectangular parallelepiped. The shorter dimension is the crystal thickness and is the dimension along the detector axis. The crystal area is defined by the longer dimensions (crystal length). The crystal area faces the source and is perpendicular to the detector axis.

It was speculated that such underestimation below 0.15 MeV could be due a crystal surface being in fact slightly larger than the nominal value and that the overestimation above 0.15 MeV could be due to a crystal's effective thickness being smaller than the nominal value.

The detector model parameters were thus fine-tuned by studying the variations in the counting efficiency when changing

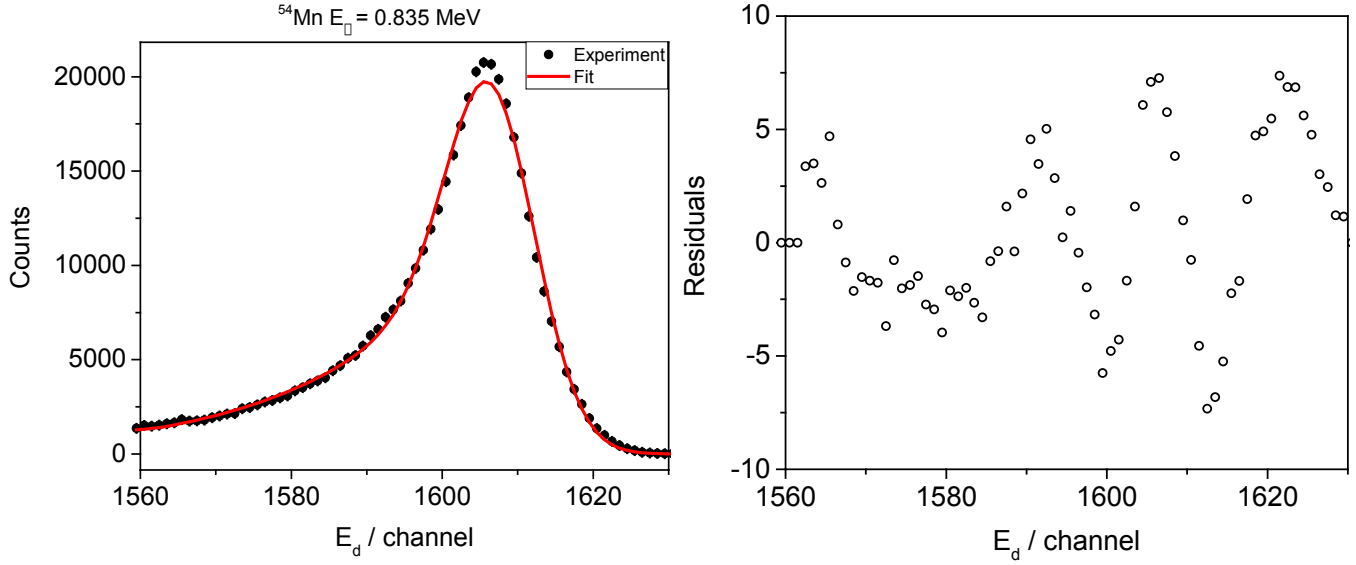

Figure 1. Result of the peak fitting procedure for the 0.835 MeV gamma-ray peak of ^{54}Mn

the linear dimensions of the crystal by up to 1 mm from their nominal values. It was found that a decrease of 1 mm in the crystal thickness starts to be have appreciable effect at 0.122 MeV where the resulting relative change in the efficiency it is about 3% and goes up to 25% at 1.3 MeV. An increase of 1 mm in the crystal length affects the gamma ray efficiency at all energies and the impact varies smoothly with gamma ray energy from 20% at 0.06 MeV to 26% at 1.3 MeV. The optimal detector model was found to have crystal dimensions of 4.0 mm x 11.2 mm x 11.2 mm, resulting in the same 500 mm^3 active detector volume as in the nominal design.

In Figure 2 the ratio between the gamma ray efficiency from the net peak areas (e_{NPA}) and the one calculated with MCNP6 (e_{MCNP}) is shown for the nominal detector design parameters and those resulting from the detector model fine-tuning.

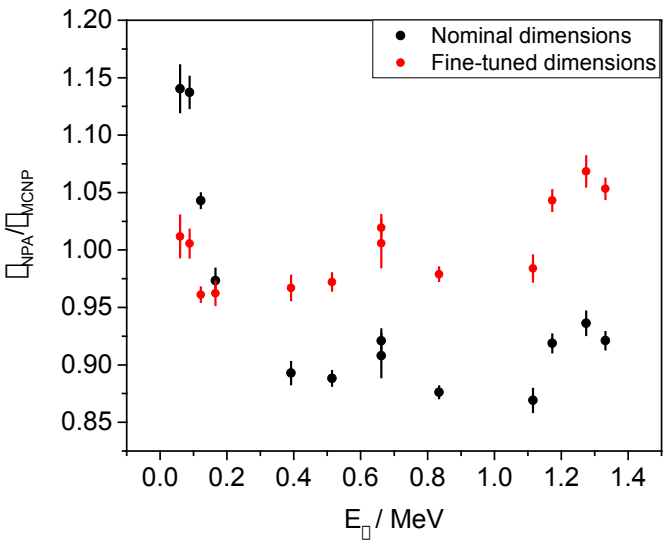

Figure 2. Ratio between the measured gamma-ray efficiency from the net peak areas (ε_{NPA}) and calculated with MCNP6 (ε_{MCNP}) are shown for the nominal and the fine-tuned crystal dimensions.

Analysis of Uranium Standards

Measurements

The considered CZT detector was used to carry out measurements of certified U_3O_8 CBNM (Central Bureau for Nuclear Measurements) EC NRM 171 standards[10] of five different values of the ^{235}U isotopic content, or enrichment, lying between 0.3%$_{wt}$ and 4.5%$_{wt}$. The measurements were carried out with a lead collimator with a cylindrical hole of 8 mm in diameter and 20 mm in length in a reproducible geometry. Due to the small detector size the infinite thickness conditions were not met.[11] A cross-sectional view of the geometry as modelled in MCNP6 is shown in Figure 3.

The maximum dead time was less than 0.03%. The measurement time ranged between 42 hours for the CBNM 446 sample and 162 hours for the 031 CBNM sample.

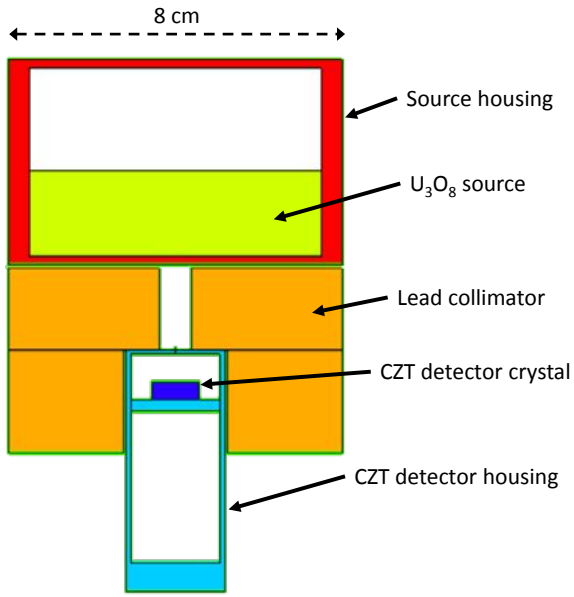

Figure 3. Cross-sectional view of the measurement geometry as modelled in MCNP 6

Spectrum Analysis

The predefined peak shape parameters were used to analyse all the spectra from the uranium standards. Only the energy calibration parameters, as well as the net peak areas, were considered as free parameters, as explained in Section 5.

The following gamma-rays of ^{235}U decay were considered in the analysis 0.143760 MeV, 0.163356 MeV, 0.185715 MeV, 0.202120 MeV, and 0.205316 MeV. In addition, we considered the gamma rays of the decay of ^{234m}Pa with which ^{238}U is in equilibrium: 0.258227 MeV, 0.742813 MeV, 0.766420 MeV, 0.786280 MeV, and 1.001030 MeV. For the data analysis of each region of interest (ROI) a background component as defined by equation no. 1 was used. At around 0.2 MeV a single ROI was considered including both the 0.202120 MeV and the 0.205316 MeV gamma lines. At around 0.76 MeV a single ROI included the triplet of gamma rays at 0.742813 MeV, 0.766420 MeV, and 0.786280 MeV.

For the data analysis required to determine the uranium enrichment, the net peak areas of the gamma rays at 0.20212 MeV and 0.205316 MeV were grouped as one data point, and so were the data in the ROI between 0.725 MeV and 0.795 MeV. The values of the net peak areas can be found in.[7]

The fit for the gamma ray spectrum of the CBNM295 sample is shown in Figure 4.

Given the fact that the measurements of the uranium

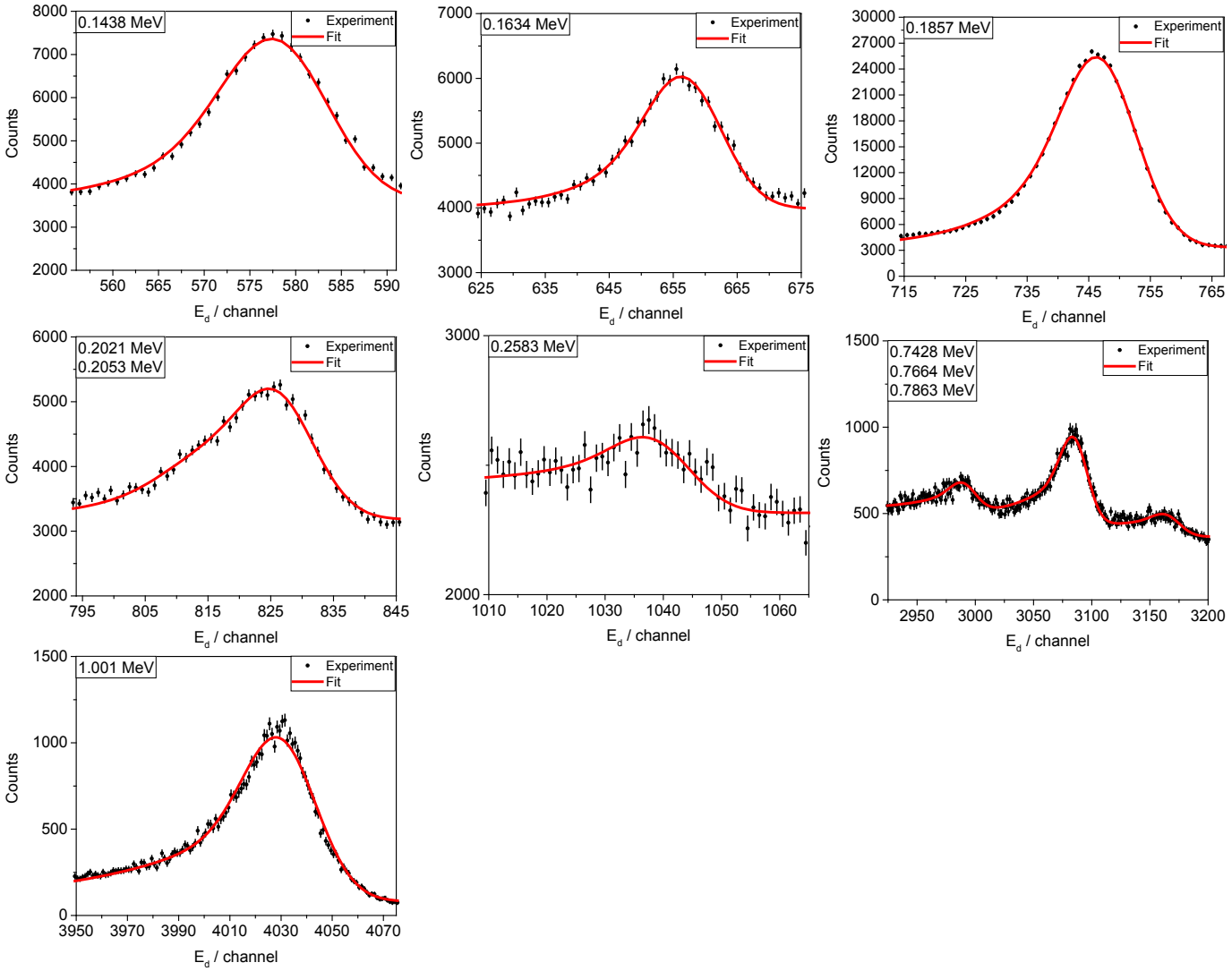

Figure 4. Fitting results for the gamma-ray spectrum of the CBNM295 sample in the seven ROIs

samples were all carried out in the same geometry conditions, we were able to verify the consistency of the net peak areas. We compared the net peak areas of all ^{235}U and ^{234m}Pa gamma rays relative to the ones of 0.1857 MeV and 1.001 MeV gamma ray, respectively.

The data reveal that the net peak areas at 0.205 MeV in the different spectra are not fully consistent with the enrichment of the samples, probably due to the low peak-to-background ratio of this peak. In addition, there is a large scatter for the area of the 0.258 MeV peak, with important differences between the CBNM071 and the CBNM194 sample.

Table 1. Relative net peak area for different CBNM samples[a]

	E / MeV	CBNM031	CBNM071	CBNM194	CBNM295	CBNM446
^{235}U	0.143760	0.159(5)	0.155(3)	0.156(2)	0.154(1)	0.154(1)
^{235}U	0.163356	0.086(4)	0.090(2)	0.088(1)	0.087(1)	0.089(1)
^{235}U	0.205316	0.136(6)	0.125(3)	0.112(2)	0.110(2)	0.116(1)
^{234m}Pa	0.258227	0.083(4)	0.059(5)	0.091(8)	0.066(6)	0.079(8)
^{234m}Pa	0.766420	0.642(7)	0.645(9)	0.617(11)	0.625(12)	0.619(14)

[a]The data for ^{235}U are relative to the 0.1857 MeV gamma ray and the data for ^{238}U are relative to 1.001 MeV gamma ray.

Implementation of the "Peak Ratio" Method

The peak ratios technique[12] is implemented for uranium enrichment determination from the analysis of high-resolution gamma spectra in codes such as FRAM.[13] With this technique it is possible to determine the relative radionuclide content in a homogenous sample, along with the relative detector efficiency, from the relative net peak areas of different radionuclides.

The application of the method requires nuclear data such as decay constants and gamma-ray emission probabilities to be known. Corrections for coincidence summing effects also need to be made wherever such effects are important. In addition, the relative counting efficiency needs to parameterized by an analytical function of gamma-ray energy, with its free parameters also determined in the fitting procedure.

In our case, calculations with the EFFTRAN code[14] were carried out to check for the importance of true coincidence summing. We concluded that true coincidence summing effects were negligible for the considered detector and counting geometry.

The peak ratio method was implemented by first calculating the quantity S_{ij} defined as equation no. 3:

$$S_{ij} = \frac{C_{ij}}{t\, I_{\gamma,ij} \lambda_j \varepsilon_{ij}},$$

as well as its associated uncertainty . In equation no. 3 *C* denotes the net peak area, *t* the measurement time I_g the emission probability, *l* the decay constant, and *e* the detector efficiency. The index *i* denotes the gamma-ray and *j* the radionuclide, respectively. The ratio between S_{ij} and N_j, where N_j is the radionuclide abundance, represents the self-absorption of gamma-rays in the sample.

We then minimized the quantity (equation no. 4):

4. $$\sum_i \left(\frac{S_{ij} - N_j g(E_i, a, b)}{u_{S_{ij}}} \right)^2$$

where *g* is an analytical function of the gamma-rayw energy E_i, with *a* and *b* as free parameters, such that the full energy peak efficiency is given as *e* ´ *g*. The function *g* therefore accounts for the absorption of gamma rays in the sample and the collimator.

In our case *j* is limited to ^{235}U and ^{238}U only and the ^{235}U isotopic content relative to ^{238}U is (equation no. 5):

5. $$k = \frac{N_{235_U}}{N_{238_U}}$$

The enrichment in percentage is then calculated as (equation no. 6):

6. $$E_{at} = 100 \frac{N_{235_U}}{N_{235_U} + N_{238_U}} = \frac{100}{1 + 1/k}$$

Monte Carlo simulations of the measurement geometry indicate that the energy dependence of the function *g* can be parameterized as (equation no. 7)[7]:

7. $$g(E, a, b) = 1 - \frac{1}{\left(1 + \left(\frac{E}{a}\right)^b\right)}$$

Nuclear Data

Nuclear data—i.e., the value of the decay constant l and the emission probabilities—enter in the definition of equation no. 2 and therefore have an impact on the results. We verified the nuclear data from four different sources for ^{235}U and ^{234m}Pa, which is in equilibrium with ^{238}U and whose gamma-rays are observed in the spectrum.

The four sources that were considered were the ENSDF evaluations,[15-17] the Nucléide–Lara Library of gamma and alpha emissions (NUCLEIDE) from Laboratoire National Henri Becquerel[18]; the 2008 IAEA handbook of nuclear data (IAEA),[19] and the Lund/LBNL Nuclear data library (LUND).[20]

The half-lives of ^{235}U and ^{238}U used in the analysis were respectively 7.038(5)´10^8 a and 4.468(5)´10^9 a. These values were the same across the four data libraries, except for the half-life of ^{235}U from the NUCLEIDE library, where its value was 7.04(1)´10^8 a.

Given the fact that detector resolution of the CZT detector is not good enough to resolve all gamma-ray peaks, the sum of the emission probabilities of the following gamma ray was used to process the corresponding net peak area:

- 0.1825 MeV and 0.1857 MeV
- 0.1989 MeV, 0.2021 MeV, and 0.2053 MeV
- 0.7400 MeV, 0.7428 MeV, 0.7664 eV, 0.7814 MeV, and 0.7863 MeV
- 0.9961 MeV and 1.001 MeV

The maximum difference in gamma-ray energy encountered was 0.06 keV for the considered gamma-rays.

The resulting emission probabilities for ^{235}U and ^{234m}Pa are given in Table 2 together with the associated gamma-ray energies that were used for the data analysis. The data for the ENSDF library are given together the percentage differences between the ENSDF data and those from the other libraries.

While the data for ^{235}U are consistent to within 1%, there are large discrepancies in the data for ^{234m}Pa. The largest inconsistencies are found for the 0.258 MeV gamma ray and the cumulative

intensity of the 0.766 MeV region.

Table 2. Emission probabilities expressed in percentages derived from the ENSDF library and percentage deviations for the other data libraries from the ENSDF values

	ENSDF			NUCLEIDE	IAEA	LUND
	Iγ			100xΔIγ/Iγ		
0.143760	10.9600	(800)		-0.2	0.0	0.0
0.163356	5.0800	(400)		0.0	0.0	0.0
0.185715*	57.3900	(3041)		0.0	+0.3	+0.3
0.205316*	6.1360	(366)		0.0	-0.7	-0.1
0.258227	0.0765	(20)		-3.6	-5.2	-4.9
0.766420*	0.4977	(43)		-1.5	-6.0	-11.2
1.001030*	0.8486	(21)		+0.5	-2.0	-0.9

Intrinsic Efficiency

The efficiency entering in equation no. 3 was obtained from the Monte Carlo detector model fine-tuned according to the description. The evaluation of the counting efficiencies from experimental data used in a previous work did not account for the fact that they were measured with a 3 mm plexiglass absorber, which was not present during the measurement with the CBNM samples.[7] Moreover, the point sources used for the parameterisation of counting efficiency were from different manufacturers and therefore had a slightly different source geometry from those in,[7] resulting in different detector-to-source distances. In the present study, the MCNP model was validated with the experimental data where both the attenuators and the detector to source distance were correctly accounted for. Therefore, the results from the fine-tuned MCNP model were considered to yield a more accurate values of the intrinsic detector efficiency and an uncertainty of 1% on the intrinsic efficiency was used in the analysis with the "peak ratio" method.

Results

We determined the enrichment for the five CBNM samples by using four different sets of nuclear data.

In addition, given the very low signal-to-background for the 0.258 MeV gamma-ray and the large scatter in the net peak area data shown in Table 1, we also analysed the data both including and excluding the net peak area of the 0.258 MeV gamma ray.

The resulting enrichments, compared to the nominal values, are given in Table 3.

Table 3. Enrichment relative to the nominal value obtained with different nuclear data sets (as indicated by the column heading), considering all available net peak areas in the analysis

	ENSDF		NUCLEIDE		IAEA		LUND	
CBNM031	1.16	(8)	1.12	(7)	1.15	(8)	1.14	(7)
CBNM071	1.37	(9)	1.32	(9)	1.45	(11)	1.36	(10)
CBNM194	1.01	(6)	0.97	(6)	0.94	(7)	0.88	(7)
CBNM295	1.14	(7)	1.11	(7)	1.11	(8)	1.09	(8)
CBNM446	1.06	(7)	1.02	(6)	1.03	(8)	0.96	(7)

The uncertainty on the enrichment is derived from the uncertainty on the input parameters by using the covariance matrix from the fit.

The enrichment of the CBNM071 sample is strongly overestimated. The data in Table 3 reveal that the ratio between the 0.258 MeV gamma rays and the 1.001 MeV is lowest for the CBNM071 samples, while the ratio is highest for the CBNM194 sample for which the enrichment is better estimated.

When excluding the 0.258 MeV gamma-ray peak from the enrichment estimation, the following results were obtained.

Table 4. Enrichment relative to the nominal value obtained with different nuclear data when excluding the net peak area of the 0.258 MeV from the analysis

	ENSDF		NUCLEIDE		IAEA		LUND	
CBNM031	1.00	(15)	0.94	(14)	0.93	(16)	0.72	(13)
CBNM071	1.03	(10)	0.97	(9)	1.01	(12)	0.76	(11)
CBNM194	1.01	(7)	0.96	(7)	0.91	(9)	0.75	(9)
CBNM295	1.00	(8)	0.96	(7)	0.88	(9)	0.73	(9)
CBNM446	1.03	(8)	0.98	(8)	0.97	(9)	0.78	(10)

Despite the fact that the uncertainty estimations of the enrichment increase when excluding the 0.258 MeV peak compared to not excluding the peak, the enrichment values obtained with ENSDF, NUCLEIDE, and IAEA data all agree within the uncertainties with the nominal value of the enrichment. When the LUND data set is used the observed bias is on average of the order of 25%. An explanation for this bias is in the 11.2% deviation of the emission probabilities for the data point at 0.766420 MeV. We do not observe such a large impact when using the IAEA data which still deviate by 6%; it is not excluded that other deviations in the IAEA data—e.g., in the emission probability of the 1.001 MeV—come into play.

The data in Table 4 do not suffer from the 10% bias that was observed in the previous evaluation.[7] In the previous study[7] the data were analysed with the ENSDF data only and using a detector efficiency that suffered from biases, as explained.

By comparing the results in Table 3 and Table 4 we can determine the impact of different nuclear data sets on the calculated enrichment. The average percentage deviations and associated standard deviation of the enrichment calculated with the NUCLEIDE, IAEA, and LUND nuclear data from the enrichment obtained with the ENSDF data are shown in Figure 5. Using the NUCLEIDE and IAEA data sets results in a systematic deviation for all the enrichments of the different samples studied. The deviation however is within the uncertainty on the enrichment. When using the LUNDL dataset a much larger deviation from the ENSDF data set results is observed. These observations are valid irrespective of whether the 0.258 MeV gamma-ray peak is used in the analysis.

In addition, the uncertainties given in Table 4 are larger than the maximum tolerable relative uncertainty value of at 7.2% for the ^{235}U enrichment quoted in.[21] The main uncertainty component is due to propagating only the counting statistics uncertainty. This component can only be reduced by increasing the measurement time or increasing the detection efficiency.

Future work will focus on studying which gamma rays, through their net peak area uncertainty, contribute the most to the obtained uncertainty on the enrichment.

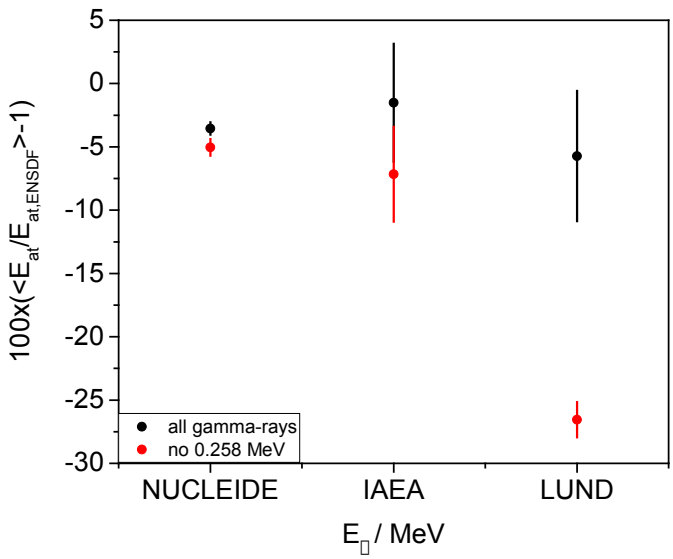

Figure 5. The average deviation in the calculated enrichment for different data libraries from the calculated enrichment with the ENSDF library and the associated standard deviation

Conclusions

We reported on the peak-shape calibration of a 500 mm^3 CZT detector. The peak shape parameters were parameterized as a function of energy by means of analytical functions and included in a peak fitting algorithm, which was then used to determine the net peak areas in spectra of five certified uranium standards.

The so-called "peak ratio" method was used to determine the uranium enrichment using a relative intrinsic detector efficiency based on Monte Carlo simulations and considering a self-absorption correction. We observed that the net peak areas of the 0.258 MeV gamma ray are not fully consistent across the five samples. We also observed that the emission probabilities of ^{234m}Pa from four different data libraries are not consistent with each other.

Our results further demonstrated that the accuracy of the 0.258 MeV net peak area bears strongly on the calculated enrichment. This is to be expected since the 0.258 MeV gamma ray defines the transition line between the ^{235}U data and the ^{234m}Pa

data regions of the spectra and hence couples the efficiency curves for these two regions. In addition, a more accurate determination of the detector efficiency over the entire energy range allowed us to remove a previously observed bias in the calculated enrichment. The uncertainty of the calculated enrichment remained such, though, that the impact of the emission probabilities on the uranium enrichment was within the calculated uncertainty, except for one of the data sets.

Alessandro Borella has a master's degree in nuclear engineering and a PhD in nuclear physics. He has worked for seven years in neutron cross-section measurements at the Institute for Reference Materials and Measurements. Since 2009 he has worked at the Belgian Nuclear Research Centre (SCK CEN) in the Nuclear Safeguards group, where he has focused on R&D work on nondestructive assay (NDA) techniques for safeguards including: Modelling, measurements and characterization of gamma-ray and neutron detectors, design optimization of detections system, neutron coincidence counting, use of cadmium zinc telluride (CZT) detectors for U and Pu verification, spent fuel measurements, data analysis with classical methods, and artificial neural networks. He has participated in international programs (e.g., ESARDA, International Partnership for Nuclear Disarmament Verification, support program to IAEA). He chaired the NDA WG of ESARDA in 2015-2017.

Michel Bruggeman received his PhD at the University of Louvain in 1990. In 1992 he joined the Belgian Nuclear Research Centre (SCK CEN) where he was responsible for setting up nondestructive assay techniques and procedures for the characterization of the nuclear wastes of SCK CEN. In 2000 he joined the Nuclear Safeguards group of SCK CEN, allowing him to further expand his expertise on nondestructive assay and with consideration to special nuclear materials, such as those in spent nuclear fuel assemblies. Currently he is head of the Low-Level Radioactivity Measurements group dealing with radioactivity analyses of environmental and bio-assay samples and is specialized in the field of gamma-ray spectrometry in laboratory applications for radioactivity determination.

Riccardo Rossa holds a master's degree and PhD in nuclear engineering. He is a research engineer at the Belgian Nuclear Research Centre (SCK CEN) with 10 years' experience in nuclear nonproliferation and safeguards. His work focuses on the development and use of nondestructive assays for the measurement of spent fuel and waste. He has also several years of experience in the application of machine learning in data analysis of spent fuel verifications. He is also actively involved in the development of safeguards approaches for various fuel cycle installations. With his work on waste characterization he is part of several European-funded projects such as CHANCE and MICADO. He is an active member of the European Safeguards Research and Development Association (ESARDA) where he is currently co-chair of the ESARDA Education and Knowledge Management (TKM) working group and will become chair of ESARDA TKM beginning January 2022.

Peter Schillebeeckx received his PhD at the University of Ghent in 1988. The subject was the investigation of fission fragment properties. He started his professional career at the Institute Lau Langevin where he was scientifically responsible for gamma-ray spectrometers. In 1989 he joined the Joint Research Centre (JRC) at Ispra, where he was scientifically responsible for the development of NDA measurement techniques based on active and passive neutron assay, gamma-ray spectroscopy, and calorimetry. Since 2001 he has been working at the JRC in Geel where he is the nuclear data group and project leader and scientifically responsible for measurements at the time-of-flight facility GELINA and tandem generator MONNET. He is specialized in cross-section measurements and the production of covariance data in the resonance region. One of his achievements is the development of an NDA technique to determine the elemental and isotopic composition of materials based on neutron resonance analysis.

Tim Vidmar earned a BSc in physics and a PhD in nuclear engineering from the University of Ljubljana, Slovenia, and subsequently worked for many years at the gamma-ray spectrometry laboratory of the Jožef Stefan Institute, a leading scientific research facility in Slovenia. Before leaving for Belgium, he was made head of that laboratory and enjoyed short post-doc stays at the PTB in Germany and the Italian National Laboratory for Ionizing Radiation. In Belgium, he worked for a year at the Institute for Reference Materials and Measurements (IRMM) on radiation metrology subjects and then joined the Belgian Nuclear Research Centre (SCK CEN) in 2009, where he spent his first year validating the functionality of the Aleph2 burnup code. In 2010 he became a member of the MYRRHA Group and has been since mainly responsible for the environmental impact assessment studies related to the MYRRHA licensing efforts. He continues to retain a keen interest in advanced topics in gamma-ray spectrometry and has developed over the years the EFFTRAN code, a freely available tool for the calculation of efficiencies and true coincidence summing correction factors in gamma-ray spectrometry that has proven popular with the practitioners of the method, especially

in developing countries. His bibliography encompasses some 80 peer-reviewed articles published in international journals, mainly on subjects of gamma-ray spectrometry and experimental and theoretical nuclear physics.

References

1. Kalemci, E., J. L. Matteson, R. T. Skelton, P. L. Hink, and K. R. Slavis. 1999. "Model Calculations of the Response of CZT Strip Detectors." In *Proceedings SPIE 3768, Hard X-Ray, Gamma-Ray, and Neutron Detector Physics*, 360. https://doi.org/10.1117/12.366601.
2. Dardenne, Y. X., T. F. Wang, A. D. Lavietes, G. J. Mauger, W. D. Ruhter, and S. A. Kreek. 1999. "Cadmium Zinc Telluride Spectral Modelling." *Nuclear Instruments and Methods in Physics Research*. A422, 159 (1999), http://dx.doi.org/10.1016/S0168-9002(98)00947-4.
3. Bolotnikov, A. E., H. Brands, G. S. Camarda, Y. Cui, R Gul, G. De Geronimo, J. Fried, A. Hossain, L. Hoy, F. Liang, J. Preston, E. Vernon, G. Yang, and R. B. James. 2016. "Cdznte Position-Sensitive Drift Detectors for Spectroscopy and Imaging of Gamma-Ray Sources." In *Proceedings of the INMM 57th Annual Meeting Conference*.
4. Arlt, R., V. Ivanov, and K. Parnham. 2000. "Advantages and Use of Cdznte Detectors in Safeguards Measurements." In *Proceedings of the MPA& C Conference*. Obninsk, Russia.
5. International Atomic Energy Agency. 2011. *Safeguards Techniques and Equipment*. Vienna, Austria: IAEA.
6. Ritec. 2013. "Spectrometric Detection Probe with Large Volume CdZnTe Detector SDP 500 (S) Operator's Manual."
7. Borella, A., M. Bruggeman, R. Rossa, and P. Schillebeeckx. 2021. "Peak Shape Calibration of a Cadmium Zinc Telluride Detector and Its Application for the Determination of Uranium Enrichment." *Nuclear Instruments and Methods*, no. 986. https://doi.org/10.1016/j.nima.2020.164718.
8. "Evaluation of Measurement Data — Guide to the Expression of Uncertainty in Measurement." 2008. *JCGM 100:2008*. 1st ed. https://www.iso.org/sites/JCGM/GUM/JCGM100/C045315e-html/C045315e.html?csnumber=50461.
9. Varnell, L., and J. Trischuk. 1969. "A Peak-Fitting and Calibration Program for Ge(Li) Detectors." *Nuclear Instruments and Methods*.
10. De Bievre, P., H. L. Eschbach, R. Lesser, H. Meyer, J. Van Audenhove, and B. S. Carpenter. 1985. "EC Nuclear Reference Material 171 Certification Report." *CEC-COM 4153*.
11. Matussek, P. 1984. "Accurate Determination of ^{235}U Isotope Abundance by Gamma Spectrometry, a User's Manual for the Certified Reference Material, EC NRM 171/NBS SRM 969." *KFK Report 3752*.
12. Harry, R. J. S., J. K. Aaldijk, and J. P. Braak. 1976. "Gamma-Spectrometric Determination of Isotopic Composition Without Use of Standards." *International Atomic Energy Agency (IAEA)*.
13. Sampson, T. 2003. "Plutonium Isotopic Analysis Using PC/FRAM." *LA-UR-03-4403*. Los Alamos, NM: Los Alamos National Laboratory.
14. Vidmar, T., G. Kanisch, and G. Vidmar. 2011. "Calculation of True Coincidence Summing Corrections for Extended Sources With EFFTRAN." *Applied Radiation and Isotopes*, 69: 908–911.
15. National Nuclear Data Center. 2015. "Evaluated Nuclear Structure Data File." Last modified September 21, 2015. https://www.nndc.bnl.gov/ensdf/DatasetFetchServlet.
16. E. Browne, J. K. Tuli. 2013. "Nuclear Data Sheets for A = 251–259 (Odd)." *Nuclear Data Sheets* 114(8-9): 751.
17. E. Browne, J. K. Tuli. 2007. "Nuclear Data Sheets for A = 137." *Nuclear Data Sheets*, 108(10): 681.
18. Laboratoire National Henri Becquerel. n.d. "Atomic and Nuclear Data." http://www.lnhb.fr/nuclear-data/module-lara/.
19. INDC International Nuclear Data Committee. 1998. "Handbook of Nuclear Data For Safeguards: Database Extensions." *INDC(NDS)-0534*.
20. Chu, S. Y. F, L. P. Ekstrom, and R. B. Firestone. 1998. "The Lund/LBNL Nuclear Data Search." http://nucleardata.nuclear.lu.se/toi/.
21. Berlizov, A., M. Koskelo, B. McGinnis, and J. Carbonaro. 2018. "Report on the Results from Phase I of the Intercomparison Exercise on U and Pu Isotopic Analysis with Medium Resolution Gamma-Ray Spectrometers (MRGS)."

SCK CEN/46654602 Rev. 1.0